RESEARCH ARTICLE

ADVANCED OPTICAL MATERIALS
www.advopticalmat.de

Strong Nonreciprocal Broadband Thermal Radiation via Materials Informatics Inverse Design

*Zihe Chen and Run Hu**

Through magneto-optical materials or spatiotemporal metamaterials, the reciprocity relation between thermal emission and absorption can be broken, achieving the more flexible nonreciprocal thermal radiation (NTR) to even approach the ultimate thermodynamic limit, such as the Landsberg limit. However, most NTR emitters only cover a narrow band, which is unwanted for thermal energy utilization. Here, a material-informatics framework with a Bayesian optimization (BO) kernel is proposed for designing NTR emitters, which consists of multilayer epsilon-near-zero (ENZ) magneto-optical films on a metal bottom. The optimal structural parameters can be obtained within only 0.5% of all possible structures, demonstrating super-efficient optimization capability. Additionally, compared to the design method based on the Fresnel formula, the broadband nonreciprocity can be significantly enhanced, with the wavelength-averaged nonreciprocity improved by 80.4%, which can be attributed to the unequal electromagnetic power dissipation density and mismatched effective impedance at opposite angles. Furthermore, the effects of the dielectric layer, different incident angles, number of layers, and magnetic fields on BO-based nonreciprocal thermal emitters have been investigated. This study can further promote the development of broadband NTR and can be extended to multilayer structures containing magnetic Weyl semimetals.

1. Introduction

All objects at nonzero temperatures spontaneously emit thermal radiation. The effective utilization of this radiative energy holds critical significance across diverse fields, including energy conversion,[1] thermal management,[2] and detection systems.[3] Recent advancements in photonic engineering have enabled the development of innovative structures and materials such as metamaterials,[4] metasurfaces,[5] photonic crystals,[6] and 2D materials,[7] offering enhanced flexibility in manipulating the spectral, directional, and polarization properties of thermal radiation. Nevertheless, most thermal emission and absorption remain fundamentally constrained by Kirchhoff's law, which dictates the equality between directional spectral emissivity and directional spectral absorptivity.[8,9] This law conventionally guides the design of thermal emitters, but it inevitably induces inherent energy losses and imposes theoretical efficiency limits in energy harvesting, such as photovoltaics and thermophotovoltaics. For instance, thermophotovoltaic systems under reciprocal constraints exhibit a maximum theoretical efficiency of 86.8%, below the nonreciprocal Landsberg limit (93.3%).[10] Consequently, breaking the constraints of Kirchhoff's law has become the holy grail for enhancing thermal energy utilization both scientifically and technologically.

As early as the 1970s, there were discussions about nonreciprocal absorption and emission.[11] In 2014, Zhu and Fan innovatively proposed a photonic crystal structure based on magneto-optical materials, theoretically achieving NTR with unequal directional spectral emissivity and absorptivity in the infrared band.[9] Since then, the concept of NTR has garnered increasing attention in various kinds of materials such as magneto-optical materials,[12–14] Kerr nonlinearity,[15,16] and time-modulated metamaterials.[17,18] However, the latter two approaches are limited by extremely complex structural requirements and very narrow nonreciprocal bandwidths. Additionally, to achieve stronger NTR, the design of NTR emitters typically requires introducing one or two resonances, such as Tamm plasmons,[19] Fabry-Perot resonances,[20,21] and guided mode resonances.[12,22] However, the coupling of single or multiple resonances usually only enables narrowband NTR at the resonance wavelength, which is not desirable for practical broadband utilization in photovoltaics and thermophotovoltaics. ENZ films can achieve wavelength and angle-selective thermal radiation by exciting Berreman modes, and constructing multilayer ENZ planar structures can enable broadband thermal radiation.[2,23,24] However, due to the isotropic dielectric tensor of traditional ENZ materials, which cannot break Lorentz reciprocity, the violation of Kirchhoff's law cannot be achieved. Recently, magnetized ENZ materials that combine

Z. Chen, R. Hu
School of Energy and Power Engineering
Huazhong University of Science and Technology
Wuhan 430074, China
E-mail: hurun@hust.edu.cn
R. Hu
Department of Applied Physics
Kyung Hee University
Yongin-si, Gyeonggi-do 17104, Republic of Korea
R. Hu
Shenzhen Institute of Huazhong University of Science and Technology
Shenzhen 518052, China

The ORCID identification number(s) for the author(s) of this article can be found under https://doi.org/10.1002/adom.202501219

DOI: 10.1002/adom.202501219

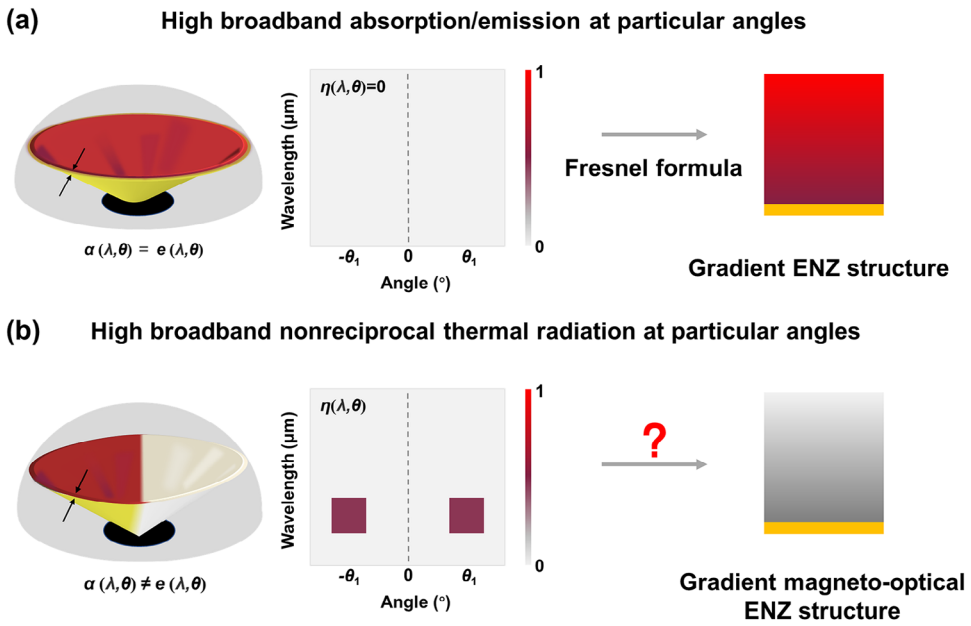

Figure 1. The schematic and effect diagrams of a) a reciprocal broadband thermal emitter based on the gradient ENZ structure and b) a nonreciprocal broadband thermal emitter based on the gradient magneto-optical ENZ structure.

magneto-optical effects and ENZ properties, such as traditional magneto-optical materials (n-InAs, InSb) or novel magnetic Weyl semimetals, have offered exciting opportunities in achieving broadband NTR.[25–27] Among these, the latter, although capable of achieving NTR without an external magnetic field due to their unique topological nontrivial electronic states and inherent time-reversal symmetry breaking, currently only realize this behavior at extremely low temperatures, without experimental verification at room temperature yet.[28] Therefore, most existing experimental demonstrations of broadband NTR rely on the utilization of traditional magneto-optical materials.[29,30] For instance, Zhao et al. proposed a multilayer nonreciprocal thermal emitter based on gradient magneto-optical ENZ materials and experimentally verified nonreciprocal broadband absorption under an external magnetic field.[28] Chen et al. theoretically demonstrated that the presence of a Fabry-Perot cavity can further enhance broadband NTR.[20] In these studies, the thickness of each ENZ material layer is typically determined using the Fresnel formula to better excite Berreman modes at the ENZ wavelength, thereby achieving stronger absorption/radiation.

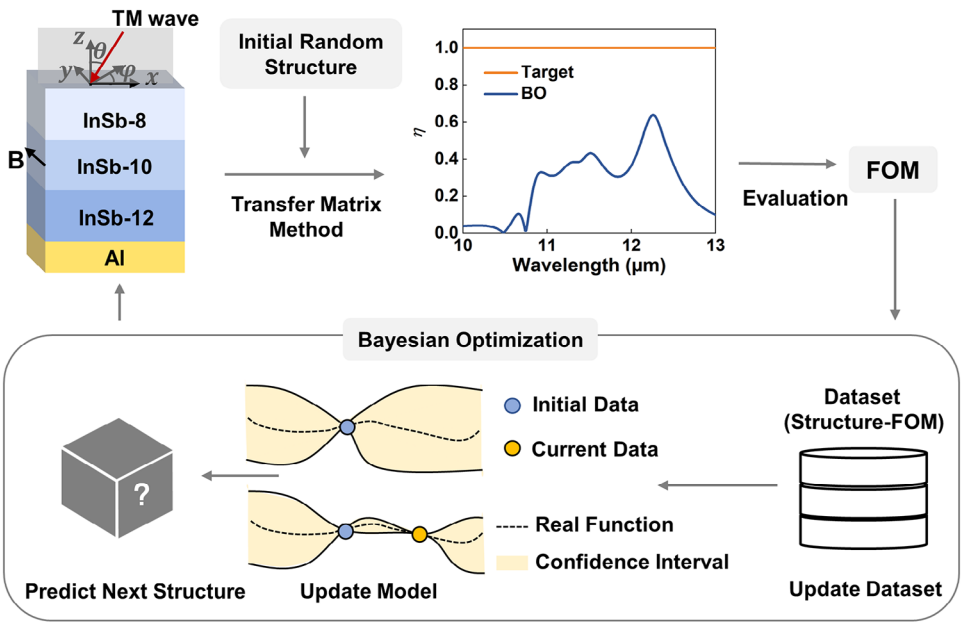

Figure 2. The design framework for nonreciprocal broadband thermal emitters.

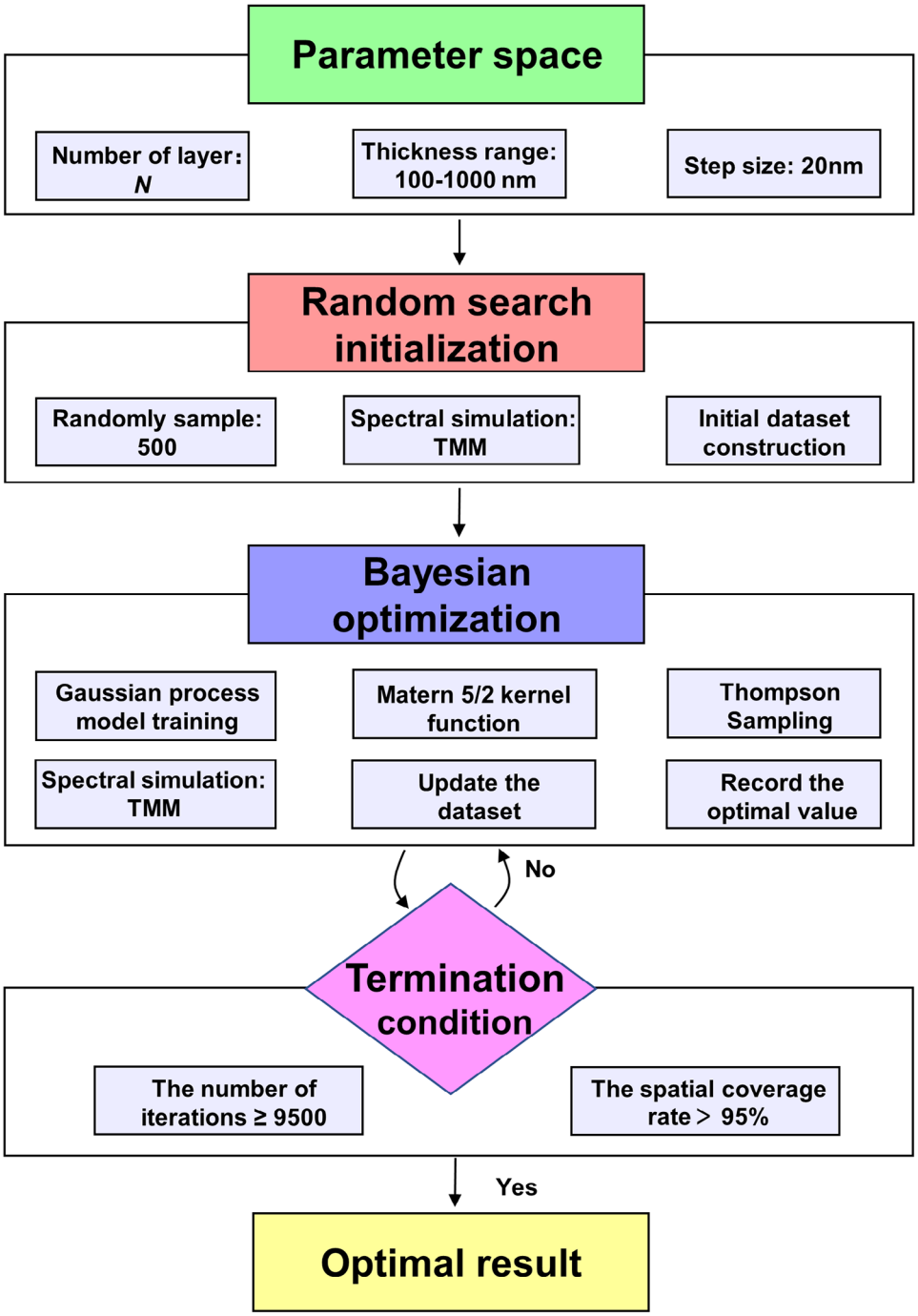

Figure 3. Flowchart based on Bayesian optimization.

However, achieving strong NTR requires maximizing the difference ($\eta = |\alpha\text{-}e|$) between the directional spectral emissivity (e) and the directional spectral absorptivity (α), not merely focusing on absorption or radiation properties. Therefore, as shown in **Figure** 1a, in reciprocal systems ($\eta = 0$), the layer thicknesses of gradient ENZ structures are typically designed using Fresnel formulas to achieve strong broadband thermal absorption/emission at particular angles, that is $\alpha = e \rightarrow 1$. However, for nonreciprocal systems aiming at strong broadband nonreciprocal thermal radiation, that is, $\eta \rightarrow 1$, whether Fresnel formulas remain applicable for designing gradient magneto-optical ENZ structures requires further investigation, as shown in Figure 1b. Moreover, strategies to achieve stronger broadband NTR remain unresolved. Fortunately, with the advancement of machine learning, materials informatics has demonstrated the capability to rapidly optimize structures and enhance performance, finding broad applications in phonon heat conduction optimization[31,32] spectral regulation,[2,33,34] and beyond. This prompts the question: Can

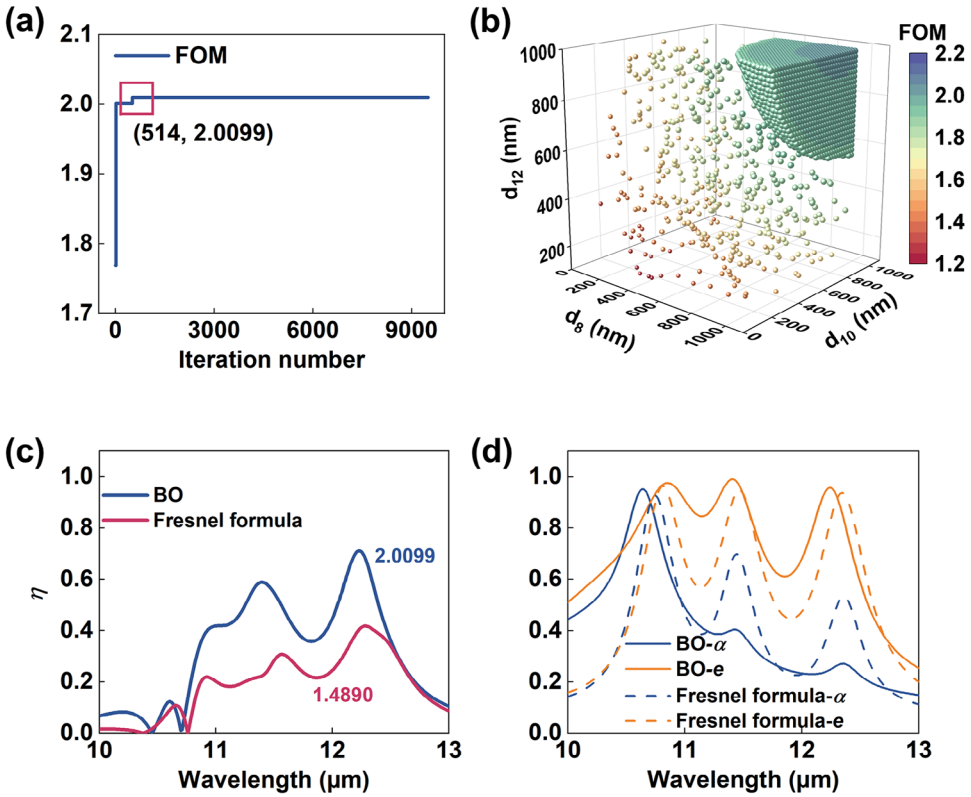

Figure 4. The optimization results for a nonreciprocal broadband thermal emitter composed of a three-layer gradient ENZ magneto-optical layer when $\theta = 70°$ and B = 3T. a) Tracing of the FOM; b) Thickness distribution of each layer during iteration; c) Comparison of nonreciprocal spectra corresponding to optimal FOM and spectra obtained by the Fresnel formula; d) The absorptivity and emissivity spectra of the BO-based nonreciprocal broadband emitter and the Fresnel formula-based nonreciprocal broadband emitter.

stronger broadband NTR be achieved by leveraging materials informatics approaches?

In this work, we present a materials-informatics framework with a BO-kernel algorithm for designing broadband NTR emitters, which comprises a three-layer gradient ENZ magneto-optical film and a bottom metal layer. Compared to conventional approaches relying on Fresnel formula-based methods, the broadband NTR here demonstrates significantly enhanced broadband nonreciprocity with an 80.4% enhancement in the average nonreciprocity within 10–13 μm. Furthermore, we also investigate the impact of varying incident angles, dielectric layer, number of layers, and magnetic field on the broadband NTR. Our results promote the development of nonreciprocal broadband thermal emitters toward more efficient and practical aspects, and are expected to develop new ways of utilizing radiation.

2. Design Methods

As shown in **Figure 2**, the nonreciprocal broadband thermal emitter consists of a gradient ENZ magneto-optical layer and a bottom aluminum layer, where the former is made of three layers ($N = 3$) of InSb with doping concentrations from top to bottom being 8, 10, and 12×10^{18} cm^{-3}. Additionally, from top to bottom, the thicknesses of each film layer are denoted as d_8, d_{10}, d_{12}, and d_{Al}, where $d_{Al} = 0.2$ μm to ensure no transmission process occurs. In addition, InSb, as a traditional magneto-optical material, requires an external magnetic field (B) to achieve NTR. When the magnetic field direction is along the *y*-axis and B = 3T, the dielectric tensor of the magneto-optical material InSb becomes asymmetric, specifically expressed as:

$$\varepsilon = \begin{bmatrix} \varepsilon_{xx} & 0 & \varepsilon_{xz} \\ 0 & \varepsilon_{yy} & 0 \\ \varepsilon_{zx} & 0 & \varepsilon_{zz} \end{bmatrix} \tag{1}$$

where

$$\varepsilon_{xx} = \varepsilon_{zz} = \varepsilon_{\infty} - \frac{\omega_p^2 (\omega + i\Gamma)}{\omega \left[(\omega + i\Gamma)^2 - \omega_c^2 \right]} \tag{2}$$

$$\varepsilon_{xz} = -\varepsilon_{zx} = -i\frac{\omega_p^2 \omega_c}{\omega \left[(\omega + i\Gamma)^2 - \omega_c^2 \right]} \tag{3}$$

$$\varepsilon_{yy} = \varepsilon_{\infty} - \frac{\omega_p^2}{\omega (\omega + i\Gamma)} \tag{4}$$

The definitions and values of symbols in Equations (1–4) can be found in Ref. [20]. Additionally, the permittivity of the bottom

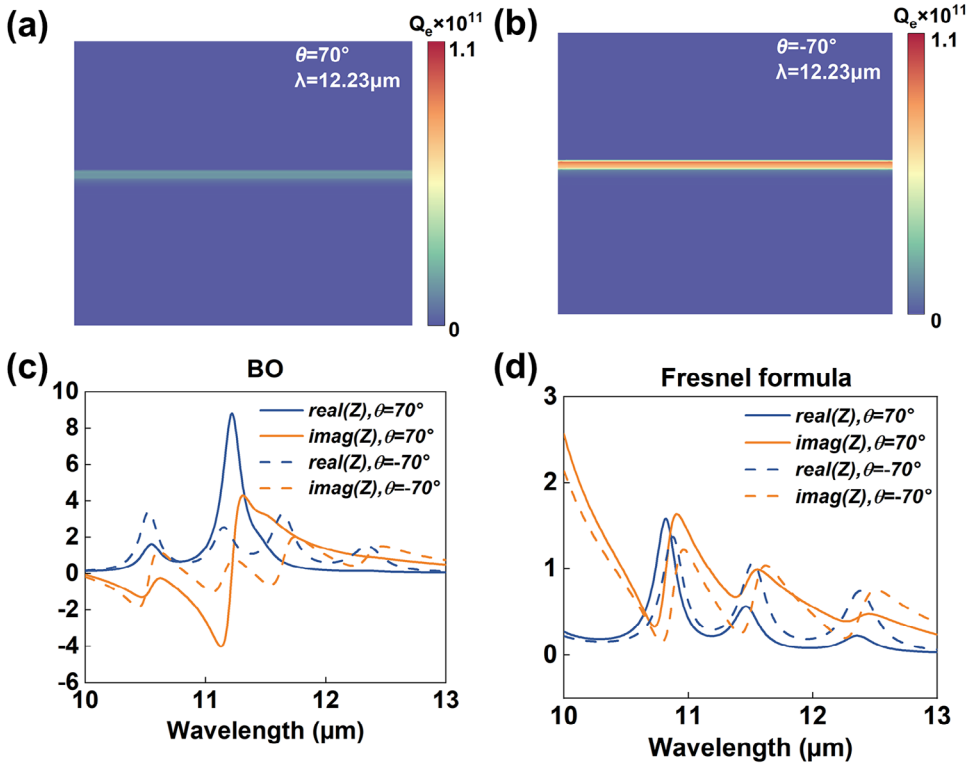

Figure 5. Mechanism analysis of strong nonreciprocal broadband thermal radiation. Distribution of electromagnetic power dissipation density within the BO-based emitter when λ = 12.23 μm: a) θ = 70°; a) θ = -70°. Effective impedance of the structure: c) BO-based emitter; d) Fresnel formula-based emitter.

aluminum layer is determined by the Drude model, expressed as:[12]

$$\varepsilon_{Al} = \varepsilon_{\infty} - \frac{\omega_p^2}{\omega(\omega + i\Gamma)} \tag{5}$$

where $\epsilon_{\infty} = 1$, $\omega_p = 2.24 \times 10^{16}$rad/s and $\Gamma = 1.24 \times 10^{14}$ rad/s.

The incident wave is a Transverse Magnetic (TM) wave, with an incidence angle of θ relative to the z-axis. When the incidence plane is rotated about the z-axis, the angle between the incidence plane and the x-axis is φ, and at this point, the rotating permittivity tensor $\overline{\overline{\varepsilon}}$ of the magneto-optical material is given by:

$$\overline{\overline{\varepsilon}} = M\varepsilon M^T \tag{6}$$

where M is represented by the rotation matrix and is given by:

$$M = \begin{bmatrix} \cos(\varphi) & \sin(\varphi) & 0 \\ -\sin(\varphi) & \cos(\varphi) & 0 \\ 0 & 0 & 1 \end{bmatrix} \tag{7}$$

Since there is no transmission process, the directional spectral emissivity and absorptivity can be expressed as functions of the directional spectral reflectivity (R), specifically:[12,21]

$$\alpha(\theta, \lambda, \varphi) = 1 - R(\theta, \lambda, \varphi) \tag{8}$$

$$e(\theta, \lambda, \varphi) = 1 - R(-\theta, \lambda, \varphi) \tag{9}$$

Here, the degree of nonreciprocity is defined as the absolute value of the difference between the directional spectral emissivity and the directional spectral absorptivity, that is:[35]

$$\eta(\theta, \lambda, \varphi) = \left| e(\theta, \lambda, \varphi) - \alpha(\theta, \lambda, \varphi) \right| \tag{10}$$

Thus, by calculating the reflection spectra of multilayer planar structures under different incident angles using the transfer matrix method (TMM), the dispersion relations for absorption, emission, and nonreciprocity can be obtained.

In reciprocal systems, to excite the Berreman mode in ENZ films for achieving strong absorption/emission, the film thickness (d_{ENZ}) is typically calculated based on Fresnel formulas, as specifically expressed:[20]

$$d_{ENZ} = \frac{\lambda_{ENZ}}{2\pi} \frac{\cos\theta}{\sin^2\theta} \left(Im\left\{ \frac{-1}{\varepsilon_{xx}} \right\} \right)^{-1}_{\max} \tag{11}$$

where λ_{ENZ} is the ENZ wavelength. However, it remains to be investigated whether the film thickness obtained through the above formula can achieve the best NTR. Therefore, optimization of the ENZ magneto-optical layer thickness is required. Here, considering an optimization range from 100 to 1000 nm with a step size of 20 nm, there are a total of 97336 possible configurations for the three-layer ENZ magneto-optical structure. In such cases, traditional manual design methods suffer from low efficiency; thus, BO algorithms are introduced in order to accelerate the design of

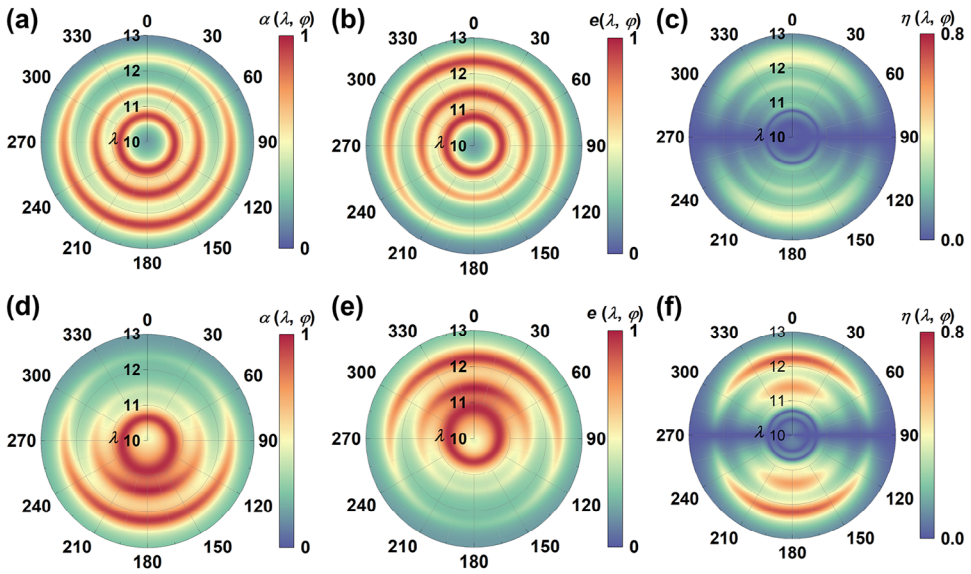

Figure 6. Spectra variation with azimuth when $\theta = 70°$ and B = 3T. Spectra of a nonreciprocal broadband thermal emitter based on the Fresnel formula: a) absorptivity; b) emissivity; c) nonreciprocity. Spectra of the optimal nonreciprocal broadband thermal emitter based on BO: d) absorptivity; e) emissivity; f) nonreciprocity.

nonreciprocal broadband thermal emitters. Here, the optimization target FOM is specifically expressed as:

$$\mathrm{FOM} = \frac{1}{MSE(\eta, \mathrm{Target})} \tag{12}$$

where MSE () represents the mean square error, the Target spectra is 1 across the wavelength range, and η is the nonreciprocity.

The design of nonreciprocal broadband thermal emitters is shown in Figure 2, and a more specific BO flowchart is shown in **Figure** 3, which includes defining the parameter space, initializing random sample search, Bayesian optimization, defining termination conditions, and outputting the optimal result.[36] First, the optimization parameter space is defined based on the three-layer gradient ENZ magneto-optical structure. The thickness range for each layer is from 100 to 1000 nm, with a step size of 20 nm. Next, randomly select 500 sets of thickness combinations from the parameter space. Based on the TMM, calculate the nonreciprocal spectrum for each thickness set, thereby obtaining the initial structure-FOM dataset. During the BO process, start by constructing a Gaussian process model based on the initial dataset. Specifically, use these randomly sampled points to predict the target value and uncertainty across the entire search space. Subsequently, based on the kernel function (Matern 5/2) and the acquisition function (Thompson Sampling), select the most promising points for further sampling and efficient computation. Add the newly obtained structure-FOM values to the existing dataset and retrain the Gaussian process model. By iteratively repeating this process until the termination criteria (The number of iterations ≥ 9500 or the spatial coverage rate > 95%) are met, the optimal structure-FOM value can be obtained, thus enabling the design of a superior nonreciprocal broadband thermal emitter.

3. Results and Discussion

Based on the design framework in Figure 2, when $\theta = 70°$, the thicknesses of each layer of the nonreciprocal broadband thermal emitter are optimized. The entire iteration process is shown in **Figure** 4a, where the horizontal axis represents the number of iterations, and the vertical axis represents the FOM value. Here, the number of iterations is 9500, accounting for ≈10% of the total possible structures. It can be seen that, when the number of iterations is 514, the FOM reaches its maximum value (2.0099), representing the optimal broadband nonreciprocity. The thicknesses of the three-layer ENZ film structure are 920, 860, and 980 nm, respectively. Additionally, the number of iterations at the optimal point accounts for 5.4% of the total iterations and only 0.5% of the total possibilities, demonstrating a high design efficiency. Figure 4b illustrates the distribution of the thicknesses of the three-layer films (d_8, d_{10}, and d_{12}), where colors approaching dark blue represent higher FOM values. In addition, larger FOM values are primarily concentrated between 600 and 1000 nm, indicating that thicknesses within this range can achieve better broadband nonreciprocity. To better highlight the superiority of this design method, a comparison is made with the nonreciprocal spectrum of a Fresnel formula-based broadband nonreciprocal emitter, as shown in Figure 4c. Here, the thicknesses of each layer, calculated based on the Fresnel formula, from top to bottom, are 310, 286, and 260 nm. The FOM value based on BO can reach 2.0099, while the result based on the Fresnel formula can only reach 1.4890. Additionally, from the nonreciprocal spectrum, it can be seen that the thermal emitter designed by BO has better broadband nonreciprocity. Figure 4d shows the absorptivity and emissivity spectra of the BO-based nonreciprocal broadband emitter and the Fresnel formula-based nonreciprocal broadband emitter. On the one hand, it can be seen that the absorption and emission spectra are separated, representing the realization of nonreciprocal thermal radiation. On the other hand,

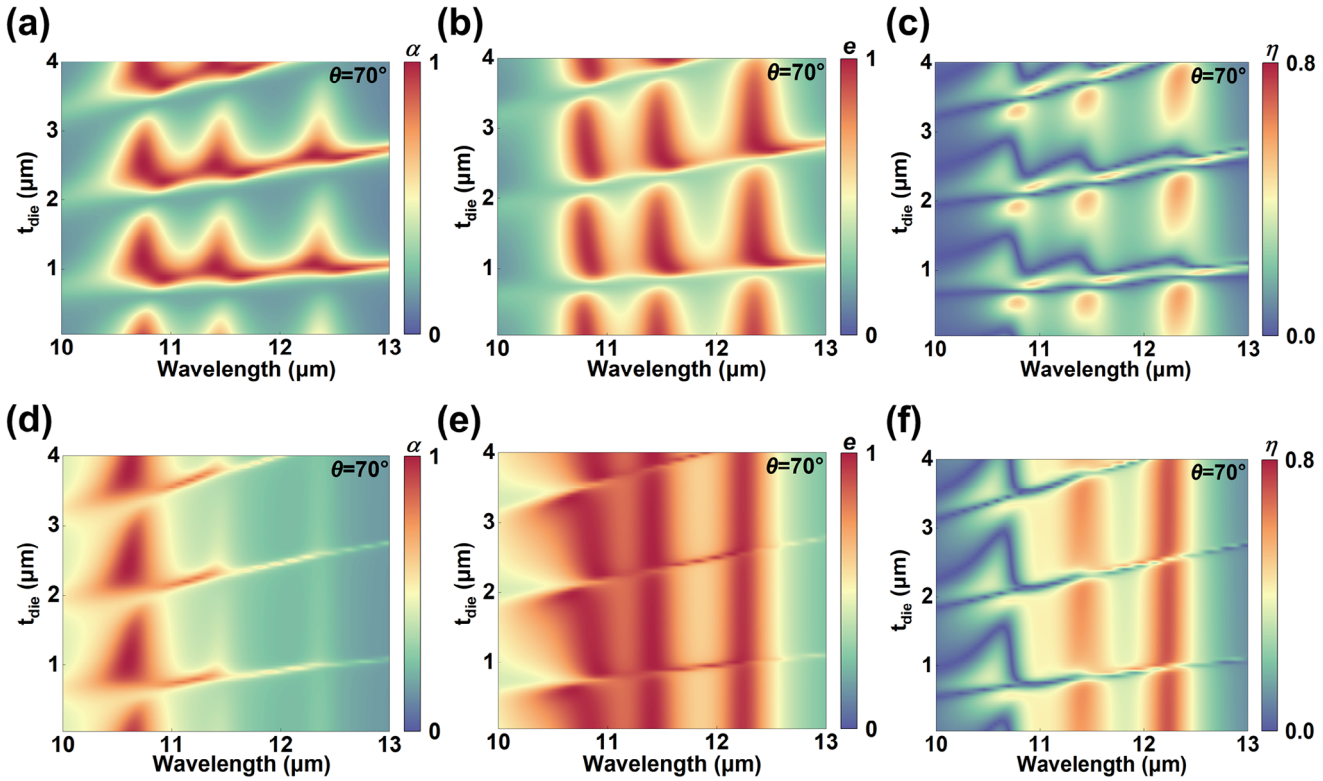

Figure 7. Spectrum variation with dielectric layer thickness with B = 3T. Spectra of a nonreciprocal broadband thermal emitter based on the Fresnel formula: a) absorptivity; b) emissivity; c) nonreciprocity. Spectra of the optimal nonreciprocal broadband thermal emitter based on BO: d) absorptivity; e) emissivity; f) nonreciprocity.

compared with the Fresnel formula-based emitter, the BO-based emitter developed in this work has a greater degree of spectral separation between absorption and emission, representing stronger broadband nonreciprocity. Here, the average nonreciprocal degree (η_{ave}) in the wavelength range (10–13 μm) is calculated. The calculation formula is:

$$\eta_{ave} = \left|\alpha_{ave} - e_{ave}\right| \tag{13}$$

where e_{ave} represents the wavelength-average emissivity and α_{ave} represents the wavelength-average absorptivity. Based on Equation (13), the average nonreciprocity of the thermal emitter designed by BO is 0.3083, while the average nonreciprocity based on the Fresnel formula is only 0.1709. The former shows an 80.4% improvement in average nonreciprocity compared to the latter. This result also demonstrates that, in nonreciprocal systems, the design method based on the Fresnel formula cannot achieve optimal broadband nonreciprocity, which is one of the key points emphasized in this work.

Next, the mechanism of nonreciprocal thermal radiation generation is analyzed, as shown in **Figure 5**. First, as shown in Figure 4c, when $\lambda = 12.23$ μm, BO-based nonreciprocal thermal emitters exhibit strong nonreciprocity ($\eta = 0.711$). Taking this wavelength as an example, the distribution of electromagnetic power dissipation density (Q_e) within the BO-based emitter structure at opposite angles is calculated, as shown in Figure 5a,b. Q_e is closely related to the absorption of the structure.[21] The larger Q_e, the stronger the absorption of the structure. It can be clearly seen that when $\theta = -70°$, this structure has a stronger Q_e, that is, a stronger absorption α (-70°) >α (70°). In addition, from Equation (9), it can be obtained that e (70°) = α (-70°). Therefore, when $\theta = 70°$, e (70°) > α (70°), demonstrating nonreciprocal thermal radiation. In addition, the impedance matching theory is adopted to further explain the reason why the nonreciprocity of BO-based emitters is stronger than that of Fresnel formula-based emitters. Here, the effective impedance matching theory is specifically expressed as:[37]

$$Z = \sqrt{\frac{\left(1 + S_{11}\right)^2 - S_{21}^{\ 2}}{\left(1 - S_{11}\right)^2 - S_{21}^{\ 2}}} \tag{14}$$

where S_{11} and S_{21} are respectively the scattering parameters related to the reflection coefficient and the transmission coefficient. The effective impedance matching theory shows that the better the effective impedance of a structure matches the free-space impedance ($Z_0 = 1$), the stronger the absorption performance of the structure. Conversely, the poorer the matching, the weaker the absorption of the structure.[37] Therefore, when the effective impedance difference of the structure at opposite angles is greater, it indicates that the absorption performance difference of the structure at opposite angles is more obvious, that is, the nonreciprocity ($\eta = |e(\theta)\text{-}\alpha(\theta)| = |\alpha(\text{-}\theta)\text{-}\alpha(\theta)|$) is stronger.

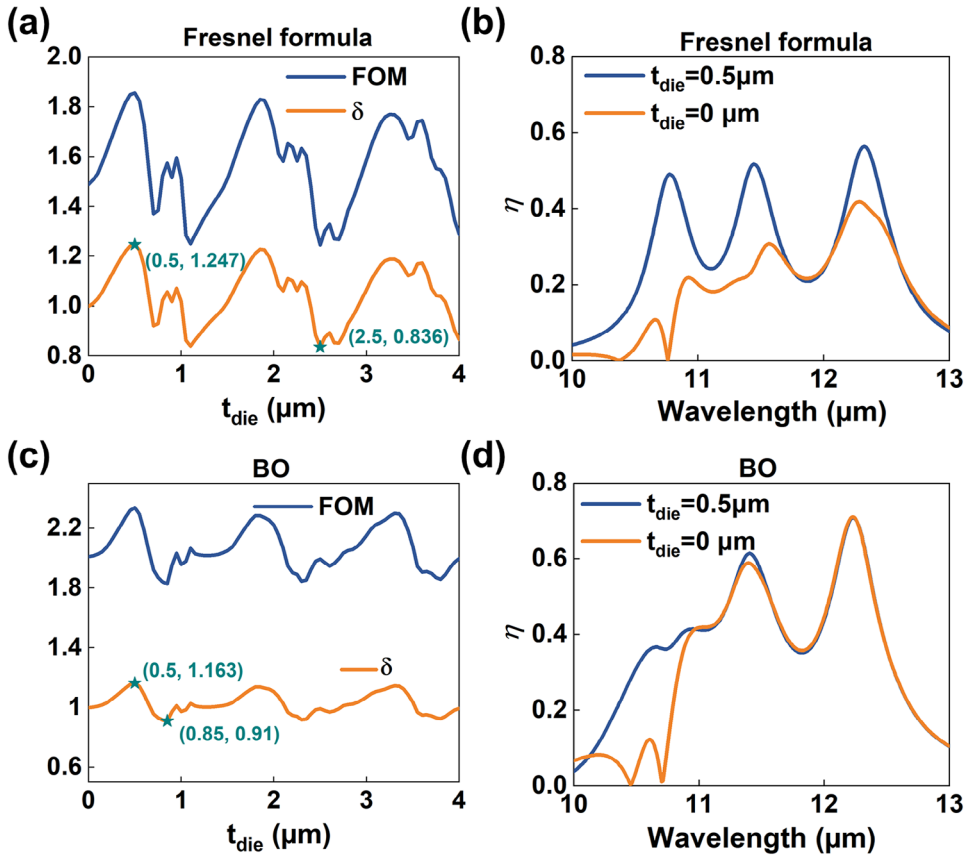

Figure 8. The nonreciprocal broadband thermal emitter based on the Fresnel formula with B = 3T: a) Variation of FOM and δ with dielectric thickness; b) The nonreciprocal spectra with t_{die} = 0.5 μm and t_{die} = 0 μm. The optimal nonreciprocal broadband thermal emitter based on BO with B = 3T: c) Variation of FOM and δ with dielectric thickness; d) The nonreciprocal spectra with t_{die} = 0.5 μm and t_{die} = 0 μm.

According to Equation (14), the impedance of the BO-based emitter and the Fresnel formula-based emitter at opposite angles (θ = 70° and θ = -70°) varies with wavelength respectively, as shown in Figure 5c,d. Taking a wavelength of 12.23 μm as an example, for the BO-based nonreciprocal emitter, Z(70°) = 0.141+1.027i and Z(-70°) = 1.05+0.432i. For the Fresnel formula-based nonreciprocal emitter, Z(70°) = 0.149+0.399i and Z(-70°) = 0.417+0.203i. It can be clearly seen that the effective impedance difference of the BO-based nonreciprocal emitter is greater at opposite angles, which also explains the reason why the BO-based nonreciprocal emitter designed in this work has stronger nonreciprocity.

Figure 6 compares the nonreciprocity of broadband thermal emitters designed by two methods as a function of azimuthal angle and wavelength. First, Figure 6a–c show the results of the thermal emitter designed by the Fresnel formulas. It can be observed that $\alpha \neq e$, indicating a violation of Kirchhoff's law. To more intuitively demonstrate the variation of nonreciprocity with the azimuthal angle, it can be seen in Figure 6c that the nonreciprocity can be realized over a wide range of azimuthal angles and presents a symmetric distribution $\approx\varphi = 90°$. Additionally, when $\varphi = 90°$, the nonreciprocity is zero. This is mainly because, at this angle, the magnetic field direction is parallel to the incident plane, causing the dielectric tensor of the magneto-optical material to have $\epsilon_{xz} = \epsilon_{zx} = 0$, meaning there is no influence from the asymmetric terms ϵ_{xz} and ϵ_{zx}. Figure 6d–f show the thermal emitter designed by BO, which, compared to Figure 6a–c, satisfies $\alpha \neq e$ while further suppressing absorption in the upper half-space (φ: 270-0°&0-90°) and emission in the lower half-space (φ: 90-180°&180-270°), thereby achieving a stronger nonreciprocity. The reason for this phenomenon may be that the more optimized thicknesses can excite a stronger asymmetric Berreman mode.[28]

In nonreciprocal systems, the presence of the dielectric layer can excite Fabry-Perot resonance, significantly enhancing nonreciprocity.[38] A similar effect also exists in nonreciprocal broadband thermal radiation structures.[20,21] However, most previous designs of nonreciprocal broadband thermal emitters were based on the Fresnel formula. Whether the BO-based nonreciprocal broadband thermal emitter designed in this work can still significantly improve nonreciprocity needs further exploration. Here, the dielectric material germanium (Ge) with a dielectric constant of 4 is selected, and its thickness (t_{die}) is explored for its impact on broadband nonreciprocity, as shown in **Figure 7**. First, for the thermal emitter optimized based on the Fresnel formula, the effects of the dielectric layer's thickness on absorption, emission, and nonreciprocity are demonstrated in Figure 7a–c. On the one hand, it can be observed that the absorption and emission spectra are distributed differently, representing a violation of Kirchhoff's law. On the other hand, the presence of the dielectric layer can periodically enhance absorption and emission, thereby periodically strengthening nonreciprocity. This is primarily due

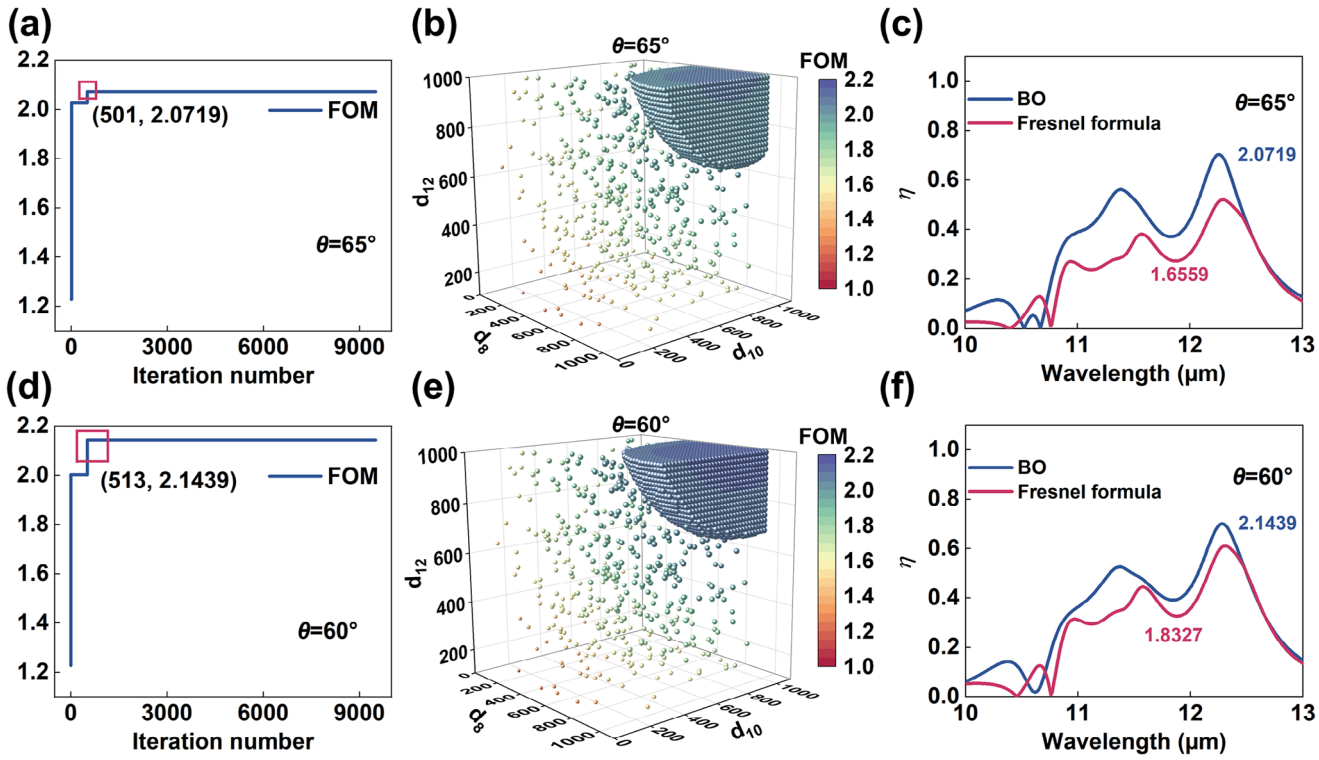

Figure 9. The optimization results for a nonreciprocal broadband thermal emitter composed of three gradient ENZ magneto-optical layers when θ = 65° and B = 3T: a) Tracing of the FOM; b) Thickness distribution of each layer during iteration; c) Comparison of nonreciprocal spectra corresponding to optimal FOM and spectra obtained by the Fresnel formula. The optimization results for a nonreciprocal broadband thermal emitter composed of three gradient ENZ magneto-optical layers when θ = 60° and B = 3T: d) Tracing of the FOM; e) Thickness distribution of each layer during iteration; f) Comparison of nonreciprocal spectra corresponding to optimal FOM and spectra obtained by the Fresnel formula.

to the dielectric layer acting as a Fabry-Perot resonance effect. As shown in Figure 7d–f, the thermal emitter with a dielectric layer optimized by BO exhibits periodic distributions as well. However, it is obvious that the nonreciprocity is stronger than the former, and the presence of the dielectric layer has a weaker effect on its nonreciprocity. Here, to more clearly demonstrate the effect of the presence of the dielectric layer on the two structures, the variation of FOM with respect to t_{die} is calculated and shown in **Figure 8**. First, for the thermal emitter designed based on the Fresnel formula, the variation of its FOM with t_{die} is presented in Figure 8a. From the overall distribution, it can be seen that the FOM fluctuates significantly with t_{die}, indicating that the presence of the dielectric layer has a substantial impact on its nonreciprocity. When t_{die} = 0.5 μm, the FOM reaches its maximum value (1.8568). When t_{die} = 2.5 μm, the FOM reaches its minimum value (1.2448). Additionally, to more clearly demonstrate the fluctuation of nonreciprocity with t_{die}, the fluctuation value (δ) is defined, and its specific expression is as follows:

$$\delta = \frac{\mathrm{FOM}\left(t_{die}\right)}{\mathrm{FOM}\left(0\right)} \tag{15}$$

where FOM(0) represents the FOM value corresponding to the nonreciprocal thermal emitter without the dielectric layer. Figure 8b compares the nonreciprocal spectra for t_{die} = 0.5 μm and t_{die} = 0 μm, showing that the presence of the dielectric layer significantly enhances the nonreciprocity of the Fresnel formula-based thermal emitter. Compared to the former, the range of δ for the BO-based thermal emitter is 0.91 to 1.163, as shown in Figure 8c, with a notably reduced fluctuation range, indicating that the dielectric layer has a weak influence on its nonreciprocity. Additionally, from the nonreciprocal spectra of the BO-based thermal emitter (Figure 8d), it can be seen that nonreciprocity is only slightly improved within the range of 10–11 μm. Therefore, compared to the Fresnel formula-based thermal emitter, the broadband nonreciprocity of the BO-based thermal emitters developed in this work is insensitive to the presence of dielectric layers. In addition, by comparing Figure 8a,c, it can be seen that even with the introduction of a dielectric layer, the maximum FOM value (1.8568) of the thermal emitter designed based on the Fresnel formula is still lower than that of the BO-based thermal emitter without a dielectric layer (2.0099), which demonstrates the superiority of the design method proposed in this work.

To further demonstrate the design flexibility of the BO-based framework method for optimizing nonreciprocal broadband thermal emitters developed in this work, the nonreciprocal broadband thermal emitters at different incident angles (θ = 65° and θ = 60°) have been optimized, as shown in **Figure 9**. First, whether at θ = 65° or θ = 60°, the maximum FOM can be quickly obtained; that is, the optimal structural parameters can be found to achieve strong broadband nonreciprocity, indicating that this method can well meet the requirements of different angles. The

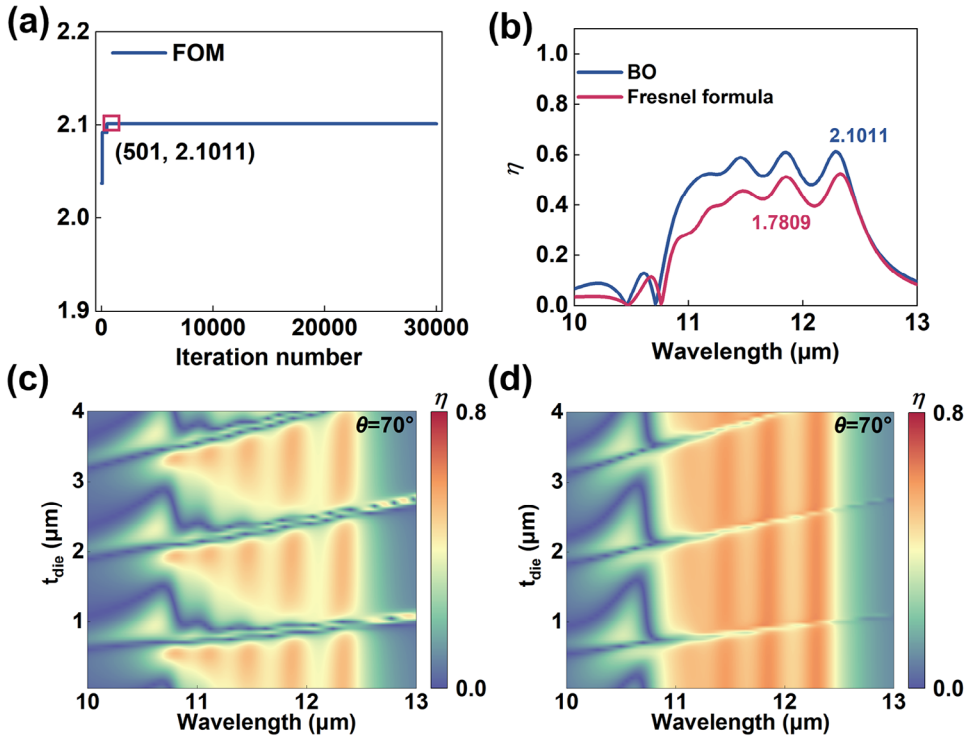

Figure 10. The optimization results for a nonreciprocal broadband thermal emitter composed of a five-layer gradient ENZ magneto-optical layer when θ=70° and B=3T. a) Tracing of the FOM; b) Comparison of nonreciprocal spectra corresponding to optimal FOM and spectra obtained by the Fresnel formula; c) Spectrum variation with dielectric layer thickness for the nonreciprocal thermal emitter based on Fresnel formula; d) Spectrum variation with dielectric layer thickness for the optimal nonreciprocal thermal emitter based on BO.

optimal thickness combinations corresponding to the maximum FOM are respectively [820, 820, 1000] and [820, 880, 1000]. In addition, by comparing the thickness-FOM distribution maps under different incident angles (Figures 4b and 9b,e), it can be seen that the larger FOM values are mainly concentrated on the upper side. Moreover, among the optimal thickness combinations corresponding to the maximum FOM values at the three angles, the thickness of d_{12} is close to 1000 nm. In other words, when optimizing more layers, the thickness of the magneto-optical ENZ at the bottom layer can be fixed at 1000 nm, thereby further enhancing the optimization efficiency of this method. Furthermore, by comparing the nonreciprocity spectra of the two design methods (Figure 9c,f), it can be seen that the BO-based thermal emitter still exhibits stronger broadband nonreciprocity, indicating that this method is highly efficient in the design of broadband nonreciprocal thermal emitters.

To further expand the number of layers in the gradient ENZ magneto-optical film to five, the doping concentrations from top to bottom are set as 8, 9, 10, 11, and $12 \times 10^{18}\mathrm{cm}^{-3}$, respectively. To simplify the number of layers optimized by BO, the thickness of d_{12} is fixed at 1000 nm, while the other four layers are optimized. The iterative process is illustrated in **Figure 10**a. It can be seen that the BO algorithm can rapidly identify the optimal FOM (2.1011) within only 501 iterations, demonstrating the high efficiency of this design method even when optimizing more layers. The optimal thicknesses corresponding to the best FOM (from top to bottom) are 640, 500, 500, 500, and 1000 nm. Additionally, by comparing the nonreciprocal spectra of the two design methods (Figure 10b), the thermal emitter designed by BO exhibits stronger nonreciprocity. Further introduction of a dielectric layer yields conclusions consistent with those for the three-layer ENZ magneto-optical film: the presence of a dielectric layer significantly enhances nonreciprocity of the Fresnel formula-based thermal emitter but provides limited improvement for the BO-based thermal emitter, as shown in Figure 10c,d.

Finally, the ability of BO to optimize nonreciprocal broadband thermal radiation under a smaller magnetic field (B = 1T) has been explored, as shown in **Figure 11**. Here, taking the three-layer magneto-optical ENZ structure as an example, the doping concentrations are 8, 10, and $12 \times 10^{18}\mathrm{cm}^{-3}$, respectively. As shown in Figure 11a, the optimization trajectory of the FOM reaches its maximum value (1.2905) at the 501st iteration, with all three magneto-optical ENZ layers optimized to a thickness of 980 nm. Figure 11b compares the absorptivity and emissivity spectra of the BO-based nonreciprocal broadband thermal emitter and the Fresnel formula-based nonreciprocal broadband thermal emitter, revealing two critical features: 1) The absorption and emission spectra do not overlap for both structures demonstrates a distinct violation of Kirchhoff's law; 2) The BO-based emitter exhibits significantly greater spectral separation, indicating enhanced nonreciprocity. To quantitatively compare their performance, Figure 11c plots the wavelength-resolved nonreciprocity, clearly demonstrating that the BO-based emitter delivers superior broadband nonreciprocity. In addition, according to Equation (13), under a 1 T magnetic field,

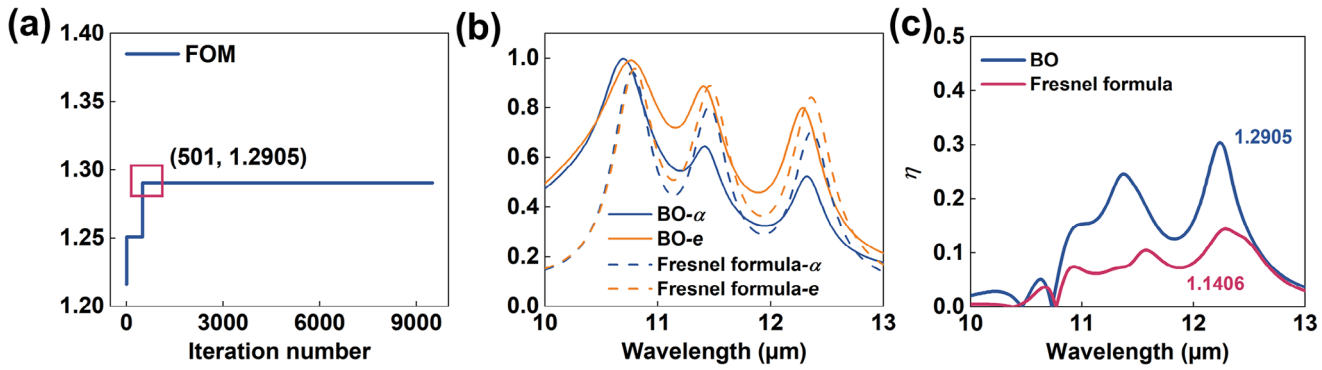

Figure 11. The optimization results for a nonreciprocal broadband thermal emitter composed of a three-layer gradient ENZ magneto-optical layer when $\theta = 70°$ and B = 1T. a) Tracing of the FOM; b) The absorptivity and emissivity spectra of the BO-based nonreciprocal broadband emitter and the Fresnel formula-based nonreciprocal broadband emitter; c) Comparison of nonreciprocal spectra corresponding to optimal FOM and spectra obtained by the Fresnel formula.

the average broadband nonreciprocity of the BO-based emitter reaches 0.1167—approximately twice that of the Fresnel formula-based emitter (0.0582). This twofold enhancement underscores the clear advantage of our BO-driven design methodology for achieving high-performance nonreciprocal broadband thermal emitters.

4. Conclusion

In summary, we propose a BO algorithm framework with materials informatics at its core to design nonreciprocal broadband thermal emitters. Compared to the traditional method, i.e., the Fresnel formulas, the designed nonreciprocal thermal emitters can achieve an increase of 80.4% in nonreciprocity, demonstrating stronger broadband nonreciprocity. This also demonstrates that the Fresnel formulas are no longer suitable for designing the thickness of the ENZ magneto-optical layer in nonreciprocal systems. Additionally, the structural parameters of the optimal nonreciprocal broadband thermal emitter only require 514 iterations, accounting for just 0.5% of the total possibilities, showcasing its fast optimization capability. Furthermore, compared to the traditional design method (Fresnel formulas), this design framework also exhibits positive design effects under different incident angles, numbers of layers, and reduced magnetic field. In addition, by introducing a dielectric layer into the nonreciprocal broadband thermal emitter, it is found that the presence of the dielectric layer has a limited impact on the nonreciprocity of BO-based thermal emitters designed in this work. Therefore, it is unnecessary to introduce a dielectric layer solely for the purpose of achieving stronger nonreciprocity, which can reduce the difficulty of fabrication to some extent. The findings of this work can promote the development of nonreciprocal broadband thermal emitters and also be extended to the optimization of multilayer structures containing Weyl semimetals.

Acknowledgements

The authors would like to acknowledge the financial support by the National Natural Science Foundation of China (52422603, 92463311, 52161160332, 52411540235), the Natural Science Foundation of Hubei Province (2023AFA072), the Interdisciplinary Research Program of HUST (5003120094), the Open Research Fund of Suzhou Laboratory (SZLAB-1508-2024-TS016), the Shenzhen Technology Project (JCYJ20241202123700001) and the Fundamental Research Funds for the Central Universities (YCJJ20242102).

Conflict of Interest

The authors declare no conflict of interest.

Author Contributions

Zihe Chen: Conceptualization, Methodology, Validation, Formal analysis, Data curation, Writing – original draft, Writing – review & editing. Run Hu: Conceptualization, Formal analysis, Writing – original draft, Writing – review & editing.

Data Availability Statement

The data that support the findings of this study are available from the corresponding author upon reasonable request.

Keywords

bayesian optimization, epsilon-near-zero, magneto-optical materials, nonreciprocal broadband thermal radiation

Received: April 17, 2025
Revised: July 11, 2025
Published online:

[1] Q. Chen, Y. Lu, J. Zhang, D. Li, T. Huang, C. Lou, M. Zhao, W. Song, H. Xu, *Nano Energy* **2023**, *114*, 108610.
[2] J.-W. Cho, Y.-J. Lee, J.-H. Kim, R. Hu, E. Lee, S.-K. Kim, *ACS Nano* **2023**, *17*, 10442.
[3] S. Yu, P. Zhou, W. Xi, Z. Chen, Y. Deng, X. Luo, W. Li, J. Shiomi, R. Hu, *Light Sci. Appl.* **2023**, *12*, 291.
[4] Z. Fan, T. Hwang, S. Lin, Y. Chen, Z. J. Wong, *Nat. Commun.* **2024**, *15*, 4544.

[5] J. Yu, R. Qin, Y. Ying, M. Qiu, Q. Li, *Adv. Mater.* **2023**, *35*, 2302478.
[6] J. S. Hwang, J. Xu, A. P. Raman, *Adv. Mater.* **2023**, *35*, 2302956.
[7] L. Zhu, F. Liu, H. Lin, J. Hu, Z. Yu, X. Wang, S. Fan, *Light Sci. Appl.* **2015**, *5*, 16052.
[8] G. Kirchhoff, *Annalen der Physik und Chemie* **1860**, *185*, 275.
[9] L. Zhu, S. Fan, *Phys. Rev. B* **2014**, *90*, 220301.
[10] Y. Park, B. Zhao, S. Fan, *Nano Lett.* **2022**, *22*, 448.
[11] R. L. Stenzel, Microwave Absorption and Emission from Magnetized Afterglow Plasmas, Ph.D. Dissertation, California Institute of Technology, Pasadena, CA **1969**.
[12] B. Zhao, Y. Shi, J. Wang, Z. Zhao, N. Zhao, S. Fan, *Opt. Lett.* **2019**, *44*, 4203.
[13] Z. Chen, S. Yu, B. Hu, R. Hu, *Int. J. Heat Mass Transfer* **2023**, *209*, 124149.
[14] Z. Chen, S. Yu, C. Yuan, X. Cui, R. Hu, *Sci. China Technol. Sci.* **2024**, *67*, 2405.
[15] A. De, A. Puri, *Appl. Phys. Lett.* **2005**, *86*, 091103.
[16] C. Khandekar, R. Messina, A. W. Rodriguez, *AIP Adv.* **2018**, *8*, 055029.
[17] A. Ghanekar, J. Wang, S. Fan, M. L. Povinelli, *ACS Photonics* **2022**, *9*, 1157.
[18] A. Ghanekar, J. Wang, C. Guo, S. Fan, M. L. Povinelli, *ACS Photonics* **2022**, *10*, 170.
[19] J. Wu, Z. Wang, B. Wu, Z. Shi, X. Wu, *Opt. Laser Tech.* **2022**, *152*, 108138.
[20] Z. Chen, S. Yu, R. Hu, *Sci. China Technol. Sci.* **2024**, *67*, 3285.
[21] K. Shi, Y. Sun, R. Hu, S. He, *Nanophotonics* **2024**, *13*, 737.
[22] Z. Chen, S. Yu, C. Yuan, X. Luo, R. Hu, *Int. J. Heat Mass Transfer* **2024**, *222*, 125202.
[23] J. Xu, J. Mandal, A. P. Raman, *Science* **2021**, *372*, 393.
[24] Y. Ying, B. Ma, J. Yu, Y. Huang, P. Ghosh, W. Shen, M. Qiu, Q. Li, *Laser Photonics Rev.* **2022**, *16*, 2200018.
[25] Z. Zhang, L. Zhu, *Phys. Rev. Appl.* **2023**, *19*, 014013.
[26] Y. Ma, J. Wang, L. Li, T. Liu, W. Li, *Laser Photonics Rev.* **2025**, *19*, 2400716.
[27] K. J. Shayegan, J. S. Hwang, B. Zhao, A. P. Raman, H. A. Atwater, *Light Sci. Appl.* **2024**, *13*, 176.
[28] M. Liu, S. Xia, W. Wan, J. Qin, H. Li, C. Zhao, L. Bi, C.-W. Qiu, *Nat. Mater.* **2023**, *22*, 1196.
[29] K. J. Shayegan, B. Zhao, Y. Kim, S. Fan, H. A. Atwater, *Sci. Adv.* **2022**, *8*, abm4308
[30] K. J. Shayegan, S. Biswas, B. Zhao, S. Fan, H. A. Atwater, *Nat. Photonics* **2023**, *17*, 891.
[31] R. Hu, S. Iwamoto, L. Feng, S. Ju, S. Hu, M. Ohnishi, N. Nagai, K. Hirakawa, J. Shiomi, *Phys. Rev. X* **2020**, *10*, 021050.
[32] S. Ju, T. Shiga, L. Feng, Z. Hou, K. Tsuda, J. Shiomi, *Phys. Rev. X* **2017**, *7*, 021024.
[33] W. Xi, Y.-J. Lee, S. Yu, Z. Chen, J. Shiomi, S.-K. Kim, R. Hu, *Nat. Commun.* **2023**, *14*, 4694.
[34] Y. Shi, W. Li, A. Raman, S. Fan, *ACS Photonics* **2017**, *5*, 684.
[35] B. Nabavi, S. Jafari Ghalekohneh, K. J. Shayegan, E. J. Tervo, H. Atwater, B. Zhao, *ACS Photonics* **2025**, *12*, 2767.
[36] Y. Motoyama, R. Tamura, K. Yoshimi, K. Terayama, T. Ueno, K. Tsuda, *Comput. Phys. Commun.* **2022**, *278*, 108405.
[37] J. Wu, Y. M. Qing, *Mater. Today Phys.* **2023**, *32*, 101025.
[38] L. Wang, F. J. García de Abajo, G. T. Papadakis, *Phys. Rev. Res.* **2023**, *5*, L022051.